Two-Step Self-Assembly of Nanodisks into Plate-Built Cylinders through Oriented Aggregation

Yao Cheng,[†] Yuansheng Wang,*[,†] Yuanhui Zheng,[†] and Yong Qin[‡]

The State Key Laboratory of Structural Chemistry, Fujian Institute of Research on the Structure of Matter, Chinese Academy of Sciences, Graduate School of Chinese Academy of Sciences, Fuzhou, Fujian 350002, China, and Institute of Solid State Physics, Chinese Academy of Sciences, Hefei, 230031, China

Received: February 4, 2005; In Final Form: April 25, 2005

Oriented aggregation-based self-assembly of hexagonal LaF_3 nanodisks with cavities into plate-built cylinders proceeding in acidic solution in the absence of any organic additive was disclosed. The self-assembly consists of two steps. First, the nanodisks sequentially aggregated together by coalescence mainly through {100} planes to form larger monocrystalline plates, followed by Ostwald ripening to smooth their surfaces. The holes on the primary nanodisks should be responsible for this intriguing growth. Second, the surface-smoothed plates were stacked face-to-face with each other along the [001] direction to construct the cylinders. The acidic condition was found to be a prerequisite for the oriented aggregations in this system.

Introduction

Solution-phase methods have been widely used for the controlled synthesis of various nanoparticles and provide models for understanding the precipitation and growth of nanoparticles. Among the crystal growth mechanisms in solution systems, the well-known Ostwald ripening, in which the growth of crystals has been thought to occur typically by atom-by-atom addition to an inorganic or organic template or by dissolution of unstable phases and reprecipitation of the more stable phase,[1] is generally believed to be the main path of crystal growth. In recent years, however, this traditional crystal growth mechanism has been challenged by the oriented aggregation mechanism, in which secondary monocrystalline particles can be obtained through attachments of primary particles in an irreversible and highly oriented fashion. Since Lee and Banfield presented this new crystal growth mechanism in 1998,[2] several kinds of organizing manners for oriented aggregation of nanocrystals have emerged. Pacholski et al. reported the formation of high-quality monocrystalline ZnO nanorods through oriented aggregation of quasi-spherical nanoparticles.[3] Liu et al. found the nanorod-directed epitaxial aggregation of $ZnWO_4$ in a solution system.[4] Either length-multiplied 1-D nanostructures or 2-D crystal sheets and walls can be obtained by self-attachment of nanorods or nanoribbons through stacking or lateral lattice fusion.[5,6] More recently, complex 3-D architectures were also developed by this self-construction mechanism through various assembly routes, for example, dendrites through 0D3D,[7,8] hollow spheres through 1D2D3D,[9] and hollow octahedrons through 0D2D3D.[10] It is deemed that, for ordered self-assembly, the aggregated nanoparticles should equilibrate with nonaggregated ones in solution, and weakly surface-protected nanoparticles often undergo entropy-driven random aggregation.[11] Therefore, for the formation of inorganic monocrystals through oriented aggregation, organic additives usually play critical roles since the binding of them to the surface of nanocrystals (building blocks) could reduce the activity of nanocrystals and thus promote ordered self-assembly.[8,11] However, a few exceptional examples dealing with oriented aggregation of nanoparticles without any organic additives came as a surprise and opened a new pathway for fabrication of novel architectures.[3,9]

Lanthanum fluoride (LaF_3) is well-known as an excellent host matrix for luminescent materials due to its low phonon energies[12] and has also been used as an extreme pressure and anti-wear additive in grease and as solid lubricant under high temperature due to its fairly low hardness, high melting point, and good resistance to thermal and chemical attack.[13] Stimulated by the nanostructure-induced peculiar properties of many inorganic nanomaterials, the interest on the preparation and the physical and chemical properties of LaF_3 nanocrystals is on the rise.[12,13] In this paper, we demonstrate a novel two-step self-assembly of LaF_3 nanocrystals. Nanodisks with holes produced in a hydrothermal system were stable in a neutral solution (pH = 7), while under acidic environment (pH = 2), they self-assembled sequentially into monocrystalline plates through crystallographically oriented aggregation, without the addition of any organic components. Furthermore, the plates stacked face-to-face with each other along a definite direction to form the 3-D cylinder-like architecture.

Experimental Procedures

The LaF_3 samples were obtained through a simple hydrothermal process. In a typical synthesis procedure, 3 mmol of KF_2H_2O was added to 10 mL of 0.1 M $La(NO_3)_3$ solution, and the pH value was adjusted by dropwise addition of dilute nitric acid. The mixture was transferred into a Teflon-lined stainless steel autoclave of 20 mL capacity. The sealed tank was heated to and maintained at 160 °C for 30 min to 20 h in an oven, then was taken out and cooled down to room temperature under ambiant conditions. The resulting white precipitates were collected by filtration and washed with deionized water and pure ethanol, respectively, several times, and then dried in air. Powder X-ray diffraction (XRD) patterns of the samples were recorded by RIGAKU-DMAX2500 X-ray diffractometer with CuKα radiation (λ = 0.154 nm) at a scanning rate of 5°/min for 2θ ranging from 5 to 85°. The morphologies and microstructures of the as-synthesized samples were characterized by field

* Corresponding author. Tel: +86-591-8370-5402; fax: +86-591-8370-5402; e-mail: yswang@fjirsm.ac.cn.
[†] Fujian Institute of Research on the Structure of Matter.
[‡] Institute of Solid State Physics.

10.1021/jp050641m CCC: $30.25
Published on Web 05/24/2005

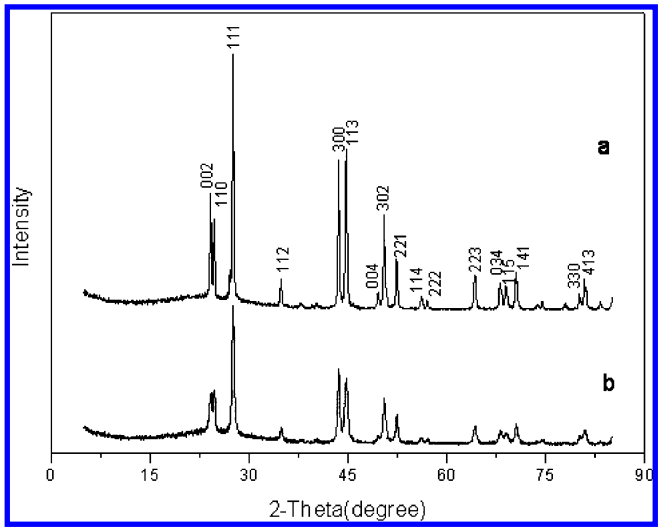

Figure 1. XRD curves of LaF_3 samples synthesized under different conditions: (a) pH = 2 and (b) pH = 7.

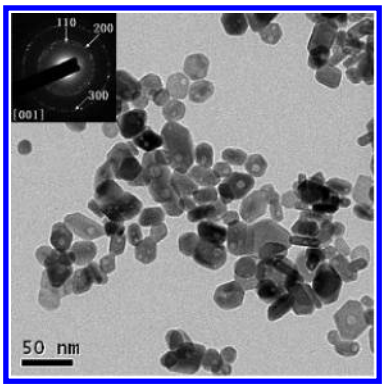

Figure 2. TEM micrograph of LaF_3 nanodisks obtained in a neutral solution (pH = 7). The inset is the corresponding SAED pattern.

emission scanning electron microscopy (FESEM, Sirion 200) at 20 kV, transmission electron microscopy (TEM, JEM-2010) at 200 kV, and selected area electron diffraction (SAED). Nitrogen isotherms at 77 K were measured using a Micromeritics ASAP 2020 apparatus. Prior to the adsorption measurements, the samples were outgassed for 5 h at 323 K.

Results and Discussion

The hexagonal LaF_3 phase (JCPDS No. 840942), which was fabricated through a hydrothermal route and identified by XRD shown in Figure 1, exhibits different morphologies. The final morphology of the as-synthesized products is determined by the pH value of the mother solution. Figure 2 is the TEM micrograph of the sample obtained in a neutral solution (pH = 7), which shows many quasi-monodispersed nanoparticles with sizes between 20 and 50 nm. Interestingly, there are one or a few cavities in each particle. Further high-resolution TEM (HRTEM) observations indicated that some cavities are half-penetrated, which is confirmed by the lattice stripes within the cavity, while others are full-penetrated for the lattice stripes halting at the margin of the cavity, as shown in Figure 3. Both corresponding fast Fourier transform patterns of the nanoparticles, shown in the insets of Figure 3a,b, are indexed as a hexagonal reciprocal lattice of the LaF_3 [001] zone axis, revealing the LaF_3 *c*-axis to be parallel to the incident electron beam. The SAED pattern in the inset of Figure 2 taken from a region consisting of many nanoparticles presents typical diffraction rings of a [001] zone axis, which is attributed to the

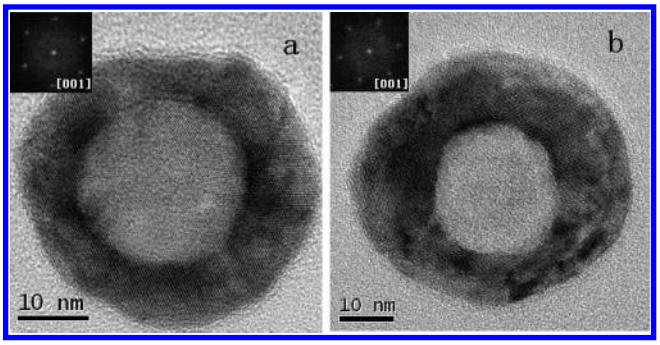

Figure 3. HRTEM images of nanodisks with (a) half-penetrated cavity and (b) full-penetrated cavity. The insets show the corresponding Fourier transform patterns.

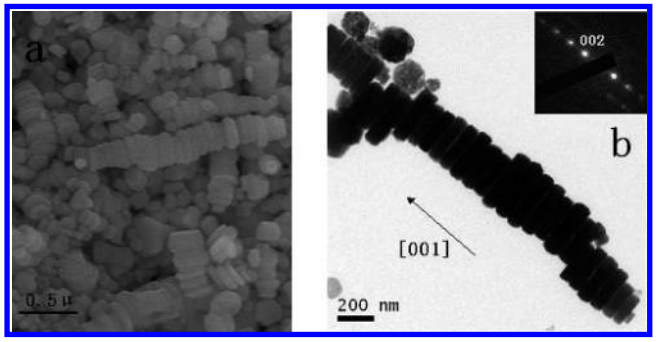

Figure 4. SEM (a) and TEM (b) micrographs of LaF_3 samples synthesized in an acidic solution (pH = 2). The inset in panel b is the SAED pattern from the center of the plate-built cylinder.

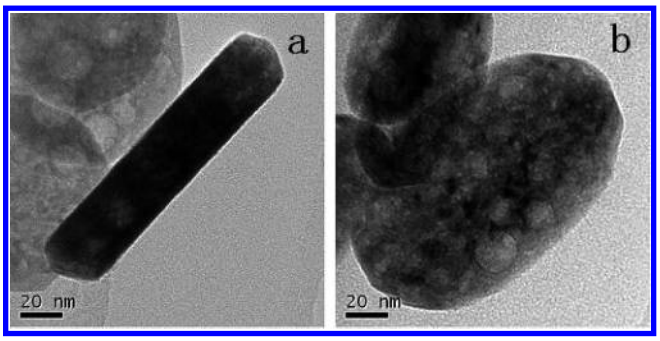

Figure 5. TEM micrographs of a standing plate: (a) before tilting and (b) sample tilted to 30.

[001] orientation consistency for all the particles (i.e., their *c*-axis is parallel to the incident electron beam while the *a*- and *b*-axis orientations are random). Therefore, it is concluded that the LaF_3 particles are of disklike morphology with the *c*-axis perpendicular to the disk's top and bottom surfaces. During aggradation of nanoparticles onto the TEM micro-grid, the nanodisks tended to lie flat on the substrate. When a hydrothermal process was performed in acidic solution (pH = 2) for 10 h, the morphology of the LaF_3 products was totally changed, as shown in Figure 4. There are many long chains of round plates, as shown in the SEM image of Figure 4a. The diameter and thickness of the plates are estimated to range from 150 to 250 nm and from 30 to 70 nm, respectively. They stack face-to-face with each other to form long chains with a length up to a few microns, which, as a whole, resemble the cylinders. In TEM images, the plate-built cylinders exhibit the morphology of chains made up of rods, for the stacked plates tend to lie on edge on the substrate. TEM tilting experiments, as illustrated in Figure 5, disclosed the actual morphology of the rods to be platelike. The extending direction of the chain is revealed by the SAED pattern (the inset of Figure 4b) to be along the [001] direction. Figure 6 shows a typical elementary unit of the cylinder: a round plate sized about

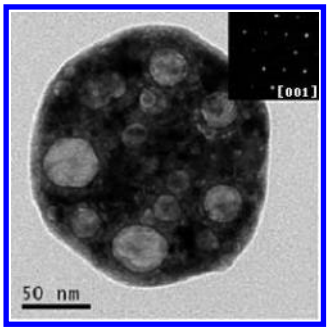

Figure 6. TEM micrograph of a surface-smoothed plate with many cavities in it. The inset shows its corresponding SAED pattern.

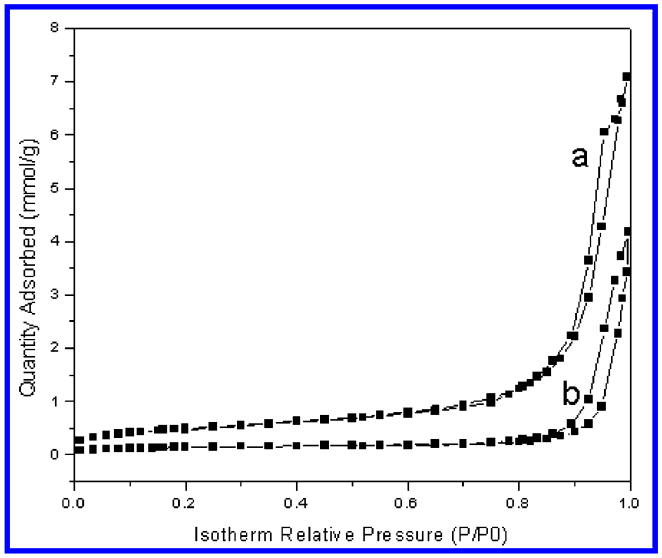

Figure 7. Nitrogen adsorption−desorption isotherms of two samples obtained under different conditions: (a) pH = 7 and (b) pH = 2.

150 nm with many cavities of different sizes in it. The plate is monocrystalline LaF_3 with its top and bottom surfaces parallel to the (001) plane confirmed by the hexagonal reciprocal lattice of the [001] zone axis of its corresponding SAED pattern. The isotherms of nitrogen adsorption and desorption for the previous two samples (pH = 7 and 2) are shown in Figure 7. Both isotherms are of a typical IV-like isotherm with hysteretic loop, indicating the presence of a certain amount of pores. Since both LaF_3 plates and nanodisks described previously exhibit similar cavity characteristics, is there any definite relationship between them? Or in other words, do the plate-built cylinders come from the nanodisks?

To uncover the formation process of the final plate-built cylinders, time-dependent experiments in acidic solution (pH = 2) were carried out, which revealed that the plates came from the self-assembly of the primary nanodisks through oriented aggregation. As shown in Figure 8, the growth of a plate started with the aggregation of a few nanodisks. Figure 8a shows the typical coalescence of two nanodisks. It is clear that, from the HRTEM image (Figure 8b) of the squared coalescent area in Figure 8a, the two nanodisks appear as clear 2-D hexagonal (001) lattice planes attached with each other through (100) planes. There are a few edge dislocations (marked by T) within the coalescent area, which is generally regarded as the consequence of oriented aggregation of particles due to small misorientation or atomic nonflatness in the interface[2] and thus marks the occurrence of particle−particle bonding. Further aggregation proceeded with the topology shown in Figure 8c: one nanodisk resided at the center with its six sides connecting with other six nanodisks, and the six sideward disks also

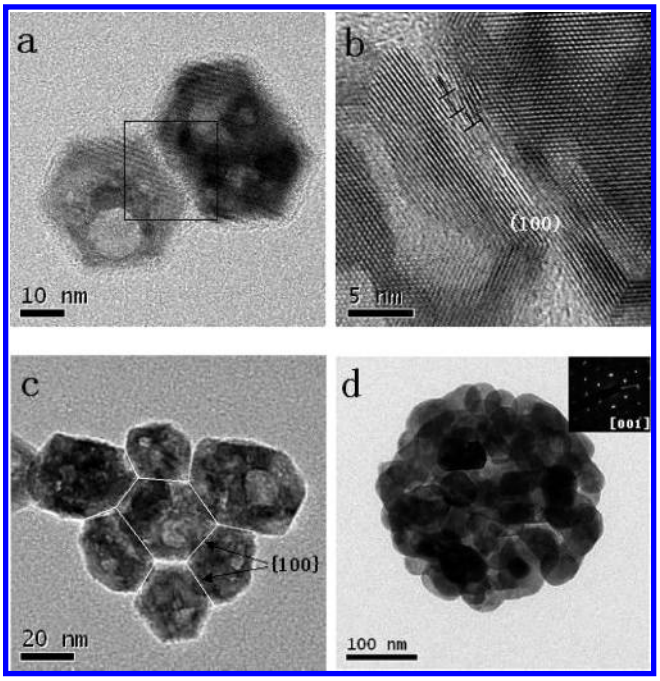

Figure 8. TEM micrographs of the congeries at different oriented aggregation stages: (a) congeries containing two nanodisks; (b) HRTEM image from the squared coalescent area in Figure 7a; (c) congeries containing several nanodisks; and (d) scabbled platelike congeries containing many nanodisks; the inset is its corresponding SAED pattern.

connected with their neighbors through {100} to reach a dense arrangement. With this process going on, the small congeries grew to the bigger one, and the aggregation seems to be not so strictly restricted within two dimensions. It extended to a few layers along the plate thickness direction, as revealed by Figure 8d. The monocrystalline SAED pattern of the plate exhibiting a hexagonal reciprocal lattice of the [001] zone axis, as shown in the inset of Figure 8d, indicates the 3-D orientational consistency for all the aggregated primary nanodisks. During the subsequent aging period, the secondary particles (i.e., the nanodisk-aggregated plates) underwent a structural modification to smooth their surfaces through traditional Ostwald ripening and finally reached the morphology as shown in Figure 6. The plates thus formed, however, were not the final architecture, and there was an obvious predisposition for them to self-assemble into cylinders by stacking face-to-face as the aging went on, as demonstrated in Figure 4. The cavities in the primary nanodisks were mostly preserved during the coalescence and smoothing processes, resulting subsequently in a porous structure of the plates and cylinders, which was consistent with the results of nitrogen adsorption and desorption experiments. Using BET methods, the surface areas and the average pore size of nanocrystals were determined to be 39 m^2/g and 22.9 nm and 11 m^2/g and 27.3 nm for samples synthesized at pH = 7 and 2, respectively. The decrease of surface area for the sample in acidic environment is due to not only the augmentation of the crystal size but also to the quantity reduction of pores on the crystal surface after aggregation. The slight increase of the average pore size indicates that some of the pores on the crystal surfaces incorporated into bigger ones during the coalescence.

The aggregation-based self-assembly from nanodisks to a plate-built cylinder is schematically illustrated in Figure 9. The result here is somewhat analogous to what has been reported for hcp-Co and Cu_2S nanodisks in the nonaqueous solutions,[14,15] where monodispersed primary nanodisks self-assembled into chains. In our system, however, the building blocks that made

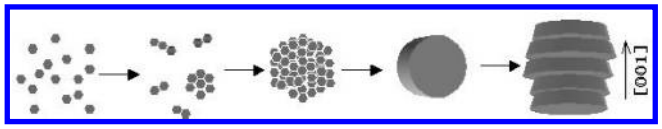

Figure 9. Schematic illustration for the self-assembly of LaF_3 nanodisks into a plate-built cylinder.

up the cylinder are not the nanodisks but are the plates aggregated previously by nanodisks. The formation of a plate-built cylinder undergoing two steps of oriented aggregation-based self-assembly has seldom been reported.

It was generally believed that the building blocks for oriented aggregations were usually nanoparticles with surfaces stabilized by organic-coating, and weakly protected nanoparticles often undergo entropy-driven random aggregation.[11] On the basis of the interaction between organic molecules and nanoparticle surfaces, the surfactant-assisted mechanisms explaining oriented aggregations of CuO,[11] $PbMoO_4$,[8] and $PbWO_4$[7] nanoparticles etc. had been proposed. In our experiment, however, the oriented aggregation of LaF_3 nanoparticles proceeded without the participation of any organic components. In addition, the acidic condition was a prerequisite for the oriented aggregations of nanodisks to form plates in this system. It is proposed that the water molecules absorbed to the LaF_3 nanodisks may work as the ligands to stabilize the primary particles and play important roles in later aggregation. It has been suggested previously that the electric field originating from a highly charged surface can align several layers of water molecules due to its semi-long-range nature.[16] It is believed that in our experiments, at acidic conditions, the positively charged LaF_3 surface, which can be attributed to some type of adsorption of cations in solution (H^+), facilitated the orientation of water molecules at the interface into a highly ordered state, while in neutral solution, the charge of the LaF_3 surface decreased due to the reduction of cations, resulting in a more random orientation of water molecules at the surface. It is easy for the primary particles containing outer water molecule layers with ordered orientation to achieve structural accord at the interface when they collide but more difficult for the ones containing a water molecule layer with random orientation. This may explain why the aggregation occurred only at acidic conditions (pH = 2) but not at neutral conditions (pH = 7). As for the oriented aggregation of primary hexagonal LaF_3 nanodisks, since the La atomic density on the (001) plane is somewhat higher than that on the {100} plane, the coalescence of nanodisks through the (001) planes seems to be energetically favored, just like the cases for the formation of hcp-Co[14] and Cu_2S[15] ribbons from nanodisks and the LaF_3 cylinder from plates in the work stated previously. From this point of view, the coalescence of LaF_3 nanodisks through the lateral {100} planes having obvious precedence over that through (001) plane is abnormal. The existence of cavities on the top and bottom surfaces of nanodisks should be responsible for it. These cavities reduce remarkably the contact area for the coalescence of two nanodisks through (001), which makes the coalescence rather weak and would enable it to be separated easily by vigorous movement and impingement of the nanoparticles in a high temperature and high pressure hydrothermal environment, thus reducing the proportion of oriented aggregation through the (001) plane. As an alternative result, the nanodisks coalesced mostly through the lateral {100} planes. At later stages of reaction, the surfaces of the plates were smoothed by the conventional Ostwald ripening, leading to an evident enlargement of the (001) contact area. This was favorable for the preferential coalescence of plates through the (001) planes, resulting in the formation of cylinders along the [001] direction. The phenomenon of cavities appearing first in nanodisks and residing in plates and plate-built cylinders is very intriguing for it extends the space of imagination for the potential application of the material. When we applied this synthesis route to other earth fluorides (e.g., NdF_3, ErF_3, and SmF_3), nanoparticles with similar cavities could always be obtained. It is thus believed that the appearance of cavities in nanoparticles should be ubiquitous for earth fluorides under this preparation condition. The formation of hollow nanocrystals is a novel and complicated process.[17] A rough explanation for the origin of pores in LaF_3 nanodisks might be the following: within the small volume of the forming nanodisks, the supersaturated vacancy cloud created somehow during the course of hydrothermal reactions is likely to coalesce into the bigger void to reduce the system energy, and this process finally resulted in the hollow structure of nanodisks. However, the detailed mechanism for the formation of cavities in earth fluoride nanoparticles is still under investigation.

Conclusion

In summary, we have demonstrated the oriented aggregation-based self-assembly of hexagonal LaF_3 nanodisks with cavities into plate-built cylinders through a surfactant-free hydrothermal route. The self-assembly consists of two steps. First, the nanodisks sequentially aggregated together by coalescence mainly through the {100} planes to form larger monocrystalline plates, followed by Ostwald ripening to smooth their surfaces. The holes on the primary nanodisks should be responsible for this intriguing growth. Second, the surface-smoothed plates stacked face-to-face with each other along the [001] direction to construct the cylinders. The acidic conditions were a prerequisite for the oriented aggregations in this system.

Acknowledgment. This work was supported by grants from the Natural Science Foundation of Fujian Province China (Project A0320001), the Ministry of Science and Technology of China (Project 2003BA323C), and the State Key Laboratory of Structural Chemistry of China (Project 050005). Helpful discussions with Dr. Jiutong Chen and Canzhong Lu are also appreciated.

References and Notes

(1) Banfield, J. F.; Welch, S. A.; Zhang, H.; Ebert, T. T.; Penn, R. L. *Science* **2000**, *289*, 751.
(2) Penn, R. L.; Banfield, J. F. *Science* **1998**, *281*, 969.
(3) Pacholski, C.; Kornowski, A.; Weller, H. *Angew. Chem., Int. Ed.* **2002**, *41*, 1188.
(4) Liu, B.; Yu, S.; Li, L.; Zhang, F.; Zhang, Q.; Yoshimura, M.; Shen, P. *J. Phys. Chem. B* **2004**, *108*, 2788.
(5) Lou, X. W.; Zeng, H. C. *J. Am. Chem. Soc.* **2004**, *125*, 2697.
(6) Liu, B.; Zeng, H. C. *J. Am. Chem. Soc.* **2003**, *125*, 4430.
(7) Liu, B.; Yu, S.; Li, L.; Zhang, Q.; Zhang, F.; Jiang, K. *Angew. Chem., Int. Ed.* **2004**, *43*, 4745.
(8) Cheng, Y.; Wang, Y.; Chen, D.; Bao, F. *J. Phys. Chem. B* **2005**, *109*, 2, 794.
(9) Liu, B.; Zeng, H. C. *J. Am. Chem. Soc.* **2004**, *126*, 8124.
(10) Yang, H. G.; Zeng, H. C. *Angew. Chem., Int. Ed.* **2004**, *43*, 5930.
(11) Zhang, Z.; Sun, H.; Shao, X.; Li, D.; Yu, H.; Han, M. *Adv. Mater.* **2005**, *17*, 42.
(12) Stouwdam, J. W.; van Veggel, F. C. J. M. *Nano Lett.* **2002**, *2*, 7, 733.
(13) Zhou, J.; Wu, Z.; Zhang, Z.; Liu, W.; Dang, H. *Wear* **2001**, *249*, 333.
(14) Puntes, V. F.; Zanchet, D.; Erdonmez, C. K.; Alivisatos, P. *J. Am. Chem. Soc.* **2002**, *124*, 12874.
(15) Sigman, M. B., Jr.; Ghezelbash, A.; Hanrath, T.; Saunders, A. E.; Lee, F.; Korgel, B. A. *J. Am. Chem. Soc.* **2003**, *125*, 5638.
(16) Gragson, D. E.; Richmond, G. L. *J. Am. Chem. Soc.* **1998**, *120*, 366.
(17) Yin, Y.; Rioux, R. M.; Erdonmez, C. K.; Hughes, S.; Somorjai, G. A.; Alivisatos, A. P. *Science* **2004**, *304*, 711.